star-forming regions, suggesting that the outer parts of the solar nebula inherited, to a large extent, the composition of the protosolar cloud (*9*). The CO depletion inferred in C/LINEAR ices might reflect their formation at higher temperatures than for Hale-Bopp, that is, closer to the Sun (*14*). However, given the small size of C/LINEAR nucleus and its high level of activity at $r_h = 4$ AU, which is better explained by CO sublimation (*5, 6*), a depletion of the CO reservoir well before perihelion cannot be excluded. The CH_3OH depletion, compared with normal abundances in species with similar volatilities (HCN), is difficult to explain by these two mechanisms.

References and Notes

1. Z. Sekanina, in *Comets*, L. L. Wilkening, Ed. (Univ. of Arizona Press, Tucson, AZ, 1982), pp. 251–287.
2. J. Chen, D. Jewitt, *Icarus* **108**, 265 (1994).
3. Z. Sekanina, *Icarus* **58**, 81 (1984).
4. J. Crovisier *et al.*, *Astron. Astrophys.* **310**, L17 (1996).
5. N. Biver *et al.*, *Science* **275**, 1915 (1997).
6. N. Biver *et al.*, *Earth Moon Planets* **78**, 5 (1999).
7. N. Biver *et al.*, *Astron. J.* **118**, 1850 (1999).
8. P. Colom *et al.*, *Earth Moon Planets* **78**, 37 (1999).
9. D. Bockelée-Morvan *et al.*, *Astron. Astrophys.* **353**, 1101 (2000).
10. W. van Driel, J. Pezzani, E. Gérard, in *High Sensitivity Radio Astronomy*, N. Jackson, R. J. Davis, Eds (Cambridge Univ. Press, Cambridge, 1996), pp. 229–232.
11. N. Biver *et al.*, *Astron. J.* **120**, 1554 (2000).
12. D. Bockelée-Morvan *et al.*, *Planet. Space Science* **42**, 193 (1994).
13. We made the assumption of steady-state isotropic outflow. OH 18-cm lines were analyzed following (*12*) with an H_2O outflow velocity assumed to be 1.0 km s^{-1}. For the species observed in the millimeter range, we used a nuclear source distribution for the local density, except for CS and H_2CO, which were assumed to come from a distributed source with parent lifetimes of $340 \times r_h^2$ s and $8000 \times r_h^2$ s, respectively (*7, 11*). The outflow velocity was estimated from the widths of the HCN lines to be 0.65, 0.7, 0.9 to 0.95, 0.75, and 0.60 km s^{-1} for the 17 to 20 June, 1 July, 18 to 23 July, 24.7 July, and 25.7 to 28.7 July periods, respectively. Rotational lines observed in the millimetric and submillimetric domains were analyzed with the excitation model of (*7, 11*), adopting a gas kinetic temperature of 50 K for June and of 70 K for July consistent with temperature determinations in low-activity comets. Beam offsets were taken into account in the calculations.
14. M. J. Mumma *et al.*, *Science* **292**, 1334 (2001).
15. T. L. Farnham *et al.*, *Science* **292**, 1348 (2001).
16. H. A. Weaver *et al.*, *Science* **292**, 1329 (2001).
17. J. T. T. Mäkinen, J.-L. Bertaux, M. R. Combi, E. Quémarais, *Science* **292**, 1326 (2001).
18. M. Kidger *et al.*, *IAU Circ. 7467* (2000).
19. The lifetime of spherical icy grains has been calculated from $\tau_d = \rho a (1 + \kappa^{-1})^{-1} r_h^2 / m_{H_2O} Z_{H_2O}$, where ρ is the grain density, a is the grain radius, κ is the gas-to-dust mass ratio, m_{H_2O} is the H_2O molecular mass, and Z_{H_2O} is the H_2O sublimation rate per unit surface at $r_h = 1$ AU. We use $Z_{H_2O} = 4 \times 10^{17}$ molecules cm^{-2} s^{-1}, corresponding to a fast rotator with geometrical albedo of 0.04. We assume ρ = 0.5 g cm^{-3} and $\kappa = 1$. At $r_h = 0.77$ AU, $\tau_d/a = 0.14$ day cm^{-1}.
20. J. F. Crifo, A. V. Rodionov, *Icarus* **127**, 319 (1997).
21. The terminal velocity of spherical grains accelerated by gas-dust momentum transfer is $V_d = 1.4\ a^{-0.5}$ $V_{\infty,exp}$ $(Q[H_2O] m_{H_2O} / 4\pi R_n \rho V_{0,exp})^{0.5}$ for a water-dominated coma. $V_{0,exp}$ and $V_{\infty,exp}$ are, respectively, the gas initial and terminal velocities, $Q[H_2O]$ and m_{H_2O} are defined in (*19*), ρ is the grain density, and R_n is the nucleus radius (*20*). Calculations of $L_d = V_d \times \tau_d$ assume $V_{0,exp} = 0.3$ km s^{-1}, $V_{\infty,exp} = 0.8$ km s^{-1} and $\rho = 0.5$ g cm^{-3}.
22. From the line intensities obtained at offset positions 10 to 15 arc sec from the nucleus on 18 to 25 July, we do not see any evidence for an extended distribution of HCN gas. Substantial departure from a nuclear source distribution is only observed on 19.6 July and is likely due to short-term variations.
23. The sublimating icy area S_{icy} is related to the H_2O production rate through $Q[H_2O] = S_{icy} Z_{H_2O}$, where Z_{H_2O} is the H_2O sublimation rate per unit surface at r_h. In the case of thermally isolated ice (model 2 in Table 2), $Z_{H_2O} = F_{sol} (1 - A)/4L_{H_2O}$, where F_{sol} is the solar flux at r_h, L_{H_2O} is the latent heat of sublimation of water ice, and A is the geometrical albedo taken equal to 0.04. In the isothermal case (model 1 in Table 2), $Z_{H_2O} = F_{sol} (1 - A)/4fL_{H_2O}$, where $f = (1 + \kappa^{-1})^{-1}$ is the icy area fraction. These equations assume a fast rotator. For computing the nucleus radius R_n, we set $4\pi R_n^2 = S_{icy}/f$.
24. We modeled the temporal evolution of the total outgassing rate of a population of icy debris, taking into account their decrease in size with time t due to sublimation according to $a(t) = a(0)(1 - t/\tau_d)$. Initial conditions are the size distribution $a^{-\alpha}$, with $a_{min} < a < a_{max}$, and the total mass at $t = 0$. The decrease of the HCN production rate observed after 23.9 July can be fitted by indexes other than $\alpha = 3.5$ but always requires that the maximum size of the debris is less than a few decimeters. Because the time sampling of our observations, the fit is not sensitive to icy grains with lifetimes smaller than one day ($a <$ 7 cm).
25. J. K. Harmon, D. B. Campbell, S. J. Ostro, M. C. Nolan, *Planet. Space Science* **47**, 1409 (1999).
26. N. Biver, thesis, Université de Paris VII (1997).
27. D. Bockelée-Morvan, T. Y. Brooke, J. Crovisier, *Icarus* **116**, 18 (1995).
28. B. G. Marsden, *IAU Circ. 6521* (1996).
29. M. Fulle, H. Mikuz, M. Nonino, S. Bosio, *Icarus* **134**, 235 (1998).
30. Compiled from the International Comet Quarterly (ICQ).
31. We thank J. Bauer and S. Sheppard for their help during the CSO observations, B. Marsden and D. Green for providing ephemerides, and J.-F. Crifo for fruitful discussions. N. Biver was supported partly by a JCMT fellowship at the University of Hawaii. This work was supported by the Programme National de Planétologie de l'Institut National des Sciences de l'Univers (INSU) and the Centre National de la Recherche Scientifique (CNRS). The JCMT is operated by the Joint Astronomy Centre on behalf of the Particle Physics and Astronomy Research Council of the United Kingdom, the Netherlands Organisation for Scientific Research, and the National Research Council of Canada. The Nançay Radio Observatory is operated by the Unité Scientifique de Nançay of the Observatoire de Paris, associated with the CNRS and also gratefully acknowledges the financial support of the Conseil Régional of the Région Centre in France. The National Radio Astronomy Observatory (NRAO) is operated by Associated Universities, under contract with the NSF. The CSO is supported by the NSF.

21 December 2000; accepted 12 March 2001

Charge Exchange–Induced X-Ray Emission from Comet C/1999 S4 (LINEAR)

C. M. Lisse,[1*] D. J. Christian,[1,2] K. Dennerl,[3] K. J. Meech,[4] R. Petre,[5] H. A. Weaver,[6] S. J. Wolk[7]

Using soft x-ray observations of the bright new comet C/1999 S4 (LINEAR) with the Chandra x-ray observatory, we have detected x-ray line emission created by charge exchange between highly ionized solar wind minor ions and neutral gases in the comet's coma. The emission morphology was symmetrically crescent shaped and extended out to 300,000 kilometers from the nucleus. The emission spectrum contains 6 lines at 320, 400, 490, 560, 600, and 670 electron volts, attributable to electron capture and radiative deexcitation by the solar wind species C^{+5}, C^{+6}, N^{+7}, O^{+7}, and O^{+8}. A contemporaneous 7-day soft x-ray light curve obtained using the Extreme Ultraviolet Explorer demonstrates a large increase in the comet's emission coincident with a strong solar flare on 14 and 15 July 2000.

Fifteen comets have now been detected in x-rays, using the BeppoSAX, Extreme Ultraviolet Explorer (EUVE), and Röntgen Satellite (ROSAT) spacecraft (*1–7*). Comparison of these results shows that (i) the emission is confined to the cometary coma between the nucleus and the Sun in a region 10^5 to 10^6 km in extent; (ii) that it is not correlated with extended dust or plasma tails; (iii) that it is not correlated in time with the solar x-ray flux; (iv) that the spectrum is soft with little C (0.28 keV) or O (0.53 keV) K-shell line emission; (v) that it is not due to scattering or resonance fluorescence or dust-dust impacts; and (vi) that all comets within 2 AU of the Sun and brighter than V = 12 were detected. The emission scales roughly as $Q_{gas}^{0.50}$, where Q_{gas} is the gas production rate from the comet, and decreases at high levels of cometary dust production, Q_{dust}. Current models (e.g., model thermal bremsstrahlung continuum with kT ~ 0.25 keV) predict a spectrum strongly increasing in intensity with increasing wavelength in the extreme ultraviolet (EUV)/soft x-ray region of the spectrum, with emission due to resonance fluorescence of solar x-rays contributing at most 20% from lines of atomic O at 530 eV and atomic C at 280 eV (*3, 4*).

Numerous potential physical mechanisms responsible for the emission have been published in the literature; all have in common an interaction between the Sun and the comet as the source of the observed x-rays. Currently, only charge exchange between highly ionized solar wind minor ions (CXE) (*2, 6–12*) and bremsstrahlung between solar wind electrons and cometary neutrals (Brem) (*2, 13–17*) are consistent with previous observations. One method to distinguish between these two emission mechanisms is to obtain a high-resolution spectrum of the emission using the Chandra ACIS-S charge-coupled device (CCD) medium-resolution spectrometers, and search for the presence of lines due to CXE emission. The CXE models of Cravens (*9*) and Wegmann *et al.* (*11*) predict multiple emission lines and an x-ray hardness maximum at the sunward edge of the emission, whereas the Brem models of Bingham *et al.* (*13, 14*) and Northrop *et al.* (*15*) predict a smooth continuum, with hardness maximum near the middle of the spatial distribution.

Here, we present conclusive evidence for detection of x-ray line emission produced by CXE in the first comet observed using the new Chandra X-ray Observatory (CXO). C/1999 S4 (LINEAR) (hereafter called C/LINEAR), a bright, actively outgassing, dynamically new comet from the Oort cloud, underwent a cataclysmic breakup in late July 2000. C/LINEAR was also an unusual comet in that it was producing a relatively large amount of cold, icy dust and carbon-poor gas as it fragmented (*18–20*), yet the comet's x-ray luminosity and morphology trends as that from previously detected, more conventional comets dominated by silicaceous dust with abundant C_n species (Fig. 1) (*2, 3*) (Web fig. 1). The similarity of C/LINEAR to the other comets in our 15-comet x-ray database argues for a gas-driven emission mechanism in the sunward side of the comet's coma, which is relatively insensitive to the gross chemical composition of the comet.

We obtained 8 pointed CXO observations (*21*) of C/LINEAR between 14 July 2000 04:30 to 08:04 UT before breakup and 16 pointings between 1 August 12:54 and 20:04 UT after breakup. The comet was approximately 0.80 AU from the Sun and 0.50 AU from Earth at the time of our study in July 2000, with total visual magnitude $\mathbf{V} = 7.5$ (*22*), $L_{optical} \sim 2 \times 10^{19}$ erg s^{-1}, and $Q_{gas} \sim 3 \times 10^{28}$ mol/s (*19, 20*). On 14 July, in 9390 s of integration, the source had a total of 13,500 counts in the 200- to 800-eV energy range after background removal, corresponding to a total x-ray luminosity of 3×10^{15} erg s^{-1} [Web fig. 1 (*23*)]. The CXO observations were coordinated with EUVE scanner observations in three filter passbands (*24*) covering the time range from 2000 July 11 22:50 UT to July 18 07:53 UT. After breakup on 1 August 2000, we again observed the comet with CXO at approximately the same heliocentric and geocentric distances and total visual brightness [V] = 7.9, but with a much more diffuse and extended optical morphology and drastically lower $Q_{gas} \sim 3 \times 10^{27}$ mol/s (*19, 20*) (Table 1). The detected CXO flux was lower by a factor of ~4, with a total of 9600 background removed counts in 18,630 s, exhibiting a highly diffuse and barely discernible emission morphology at the 4σ confidence level. At much lower SNR than the July observa-

[1]University of Maryland, Department of Astronomy, College Park, MD 20742, USA. [2]Computer Sciences Corporation, Science Operations, 3700 San Martin Drive, Baltimore, MD 21218, USA. [3]Max-Planck-Institut für Extraterrestrische Physik, Postfach 1603, 85740 Garching, Germany [4]Institute for Astronomy, University of Hawaii, 2680 Woodlawn Drive, Honolulu, HI 96822, USA. [5]Code 666, NASA Goddard Spaceflight Center, Greenbelt, MD 20771, USA. [6]Johns Hopkins University, Department of Physics and Astronomy, 3400 North Charles Street, Baltimore, MD 21218, USA. [7]Chandra X-Ray Center, Harvard-Smithsonian Center for Astrophysics, 60 Garden Street, Cambridge, MA 02138, USA.

*To whom correspondence should be addressed. E-mail: lisse@astro.umd.edu

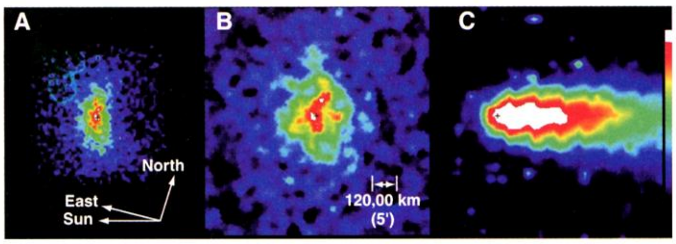

Fig. 1. X-ray and EUVE Images of C/LINEAR. **(A)** Chandra 0.20- to 0.80-keV ACIS-S 14 July 2000 image and **(B)** EUVE 0.09- to 0.25-keV (Lexan B) scanner telescope 13 to 15 July 2000 image. **(C)** Visible light image of the comet taken on 14 July 2000 UT, demonstrating a symmetric coma with a long, narrow, antisolar tail. The images are in a reference frame moving with the comet's apparent sky position. The position of the comet's nucleus is denoted by a "+". The projected direction toward the Sun is to the left in each image, with an effective spatial resolution of 10″ or 4000 km/pixel. To produce the highest contrast, the emission intensity has been normalized in each individual image so that the maximum intensity, denoted by the color white, has the value 255 (color bar on right).

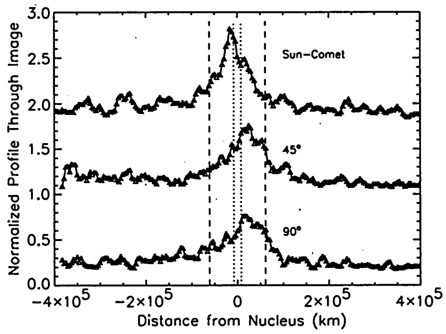

Fig. 2. Profiles of the 13 to 15 July 2000 UT EUVE image of the comet. The profiles have been offset vertically for presentation purposes. The profiles at −45° (not shown) are similar to the +45° profile, demonstrating the symmetry of the emission about the nucleus. The error bars are ±2σ. Vertical lines indicate radial position of the comet's bowshock, assuming that the position is proportional to Q_{gas} (dotted vertical lines) or $Q_{gas}^{1/2}$ (dashed vertical lines).

Table 1. Position, gas production rate, and approximate radial extent of the observed x-ray emission for C/LINEAR and previous well-measured comets. Here, r_h is the comet-Sun distance; Δ is the comet-Earth distance; the heliographic latitude and Δ*Longitude* = (*Longitude*$_{Comet}$ − *Longitude*$_{Earth}$) are the comet's position as seen from the Sun; and Q_{gas} is the gas production rate from the nucleus surface.

Comet	Date (00:00H UT)	r_h (AU)	Δ (AU)	Heliographic latitude, Δ*longitude* (deg)	Q_{gas} (mol s^{-1})	Measured extent (km)
Hyakutake (*1*)	27 Mar 1996	1.01	0.12	+1, −3.4	2×10^{29}	1-2 × 10^5
Hyakutake (*2*)	22 Jun 1996	1.33	1.2	−47, +26	1×10^{29}	~1 × 10^6
Encke (*2*)	7 Jul 1997	1.04	0.19	−4, −3.9	2×10^{27}	~5 × 10^4
Levy (*3*)	7 Sep 1990	1.25	0.57	+5, −27	2×10^{29}	~1 × 10^6
Hale-Bopp (*6*)	11 Sep 1996	3.1	2.9	+22, −68	6×10^{29}	~1 × 10^6
d'Arrest (*7*)	4 Sep 1995	1.4	0.46	−3, +4.0	1×10^{28}	1 × 10^5
TT (*18*)	10 Jan to 03 Feb 1998	1.26 to 1.06	0.45 to 0.71	+15.9 to +11.4, +10.8 to −38.3	3×10^{27}	~1 × 10^5
LINEAR	11 to 18 Jul 2000	0.82 to 0.78	0.64 to 0.41	+33 to +29, +30 to +9	3×10^{28}	~3 × 10^5
LINEAR	1 Aug 2000	0.77	0.56	+14, −32	~4 × 10^{27}	>2 × 10^5*

*No radial extent discernible in the ACIS-S field of view after breakup.

tions, the postbreakup August observations serve mainly as a test of the emission mechanism dependence on Q_{gas} and Q_{dust}, and of the constancy of the spectral emission.

The emission morphology is crescent shaped, extending out to about 100,000 km (4′ at 0.6 AU) in radius (Fig. 1), and centered around the Sun-nucleus line, within the positional errors of our measurement, similar to that found for previous comets. Spatial brightness profiles of the emission are more extended perpendicular to the Sun-nucleus line than in other directions (Fig. 2). The EUVE image, at about three times lower angular resolution, shows a similar morphology in the highest signal regions, although it is asymmetric far from the nucleus. The measured 90% extent of the CXO image, 100,000 km, is smaller than expected for the trend line found for previous EUVE and ROSAT comets. The 90% extent of the EUVE image is, by contrast, 300,000 km. The difference is due to the 8.3′-wide CXO versus the 5°-wide EUVE instantaneous fields of view: the reconstructed CXO map is highly vignetted at the edges, and the comet overfills the S3 chip (Fig. 1). We thus adopt the EUVE spatial profiles for the full extent of the comet, and correct the estimated CXO total count rates for the amount of x-ray flux that has fallen outside of the field of view. Images of the comet emission taken in four 50 eV wide bandpasses centered at 360, 450, 560, and 660 eV demonstrate no clear difference in the radial extent versus photon energy—there is no clear trend in hardness with distance from the comet's nucleus—but this may be an effect of the overfilling of the CCD chip, because the extremes of the comet's emission are poorly sampled in our reconstructed image.

The hemispherical emission geometry is consistent with a cometary extended atmosphere encountering the solar wind, fully depleting the population of minor ions in charge exchange interactions, before the wind travels through to the antisolar side of the coma. The total observed x-ray luminosity is near the maximum measured for any comet (*2, 3*) (Web fig. 1A), even though C/LINEAR was six times less active than C/Hyakutake and 30 times less active than C/Hale-Bopp (Table 1). This strongly suggests the active emitting area is restricted to a radius of less than 5×10^5 km from the comet's nucleus by some means, with the most likely restricting process, given CXE-driven emission, being the length scale for solar UV photoionization of neutrals in the cometary coma. Like other comets at 1 AU, the gas emission from LINEAR S4 was dominated by an outflow of water. The length scale for significant ionization in a water-dominated coma is on the order of $\tau_{H_2O,ionize} \sim 1 \times 10^6$ s * 0.8 km s^{-1} gas outflow rate = 8×10^5 km.

The position of the subsolar bowshock and contact surface for C/LINEAR during our observations can be inferred from the P/Halley in situ magnetic field measurements (*25*), scaling the distances by the factor Q_{gas} for each comet (*1, 2, 26*). Using a gas production rate for Halley of $\sim 1 \times 10^{30}$ mol s^{-1} and a subsolar bowshock distance of 5×10^5 km (*27–29*), we find for C/LINEAR on 14 July 2000, with $Q_{gas} \sim 3 \times 10^{28}$ mol s^{-1}, a subsolar bowshock distance of 11,000 km. Thus, the majority of detected x-ray photons are emitted outside the comet's bowshock (*30*) (Fig. 2, Web fig. 1B), and there is no obvious discontinuity or enhancement of the observed emission in our images. This strongly suggests that the observed emission does not depend critically on the local magnetic field strength in the coma, and is consistent with a CXE driven emission mechanism.

The 200- to 800-eV CXO spectrum of the cometary emission on 14 July deviates from a simple continuum, demonstrating multiple features, including pronounced lines at 400, 560, and 660 eV, and rises toward low energies (Fig. 3). Fits were made to the spectrum with several simple continuum models previously used to describe lower resolution x-ray data and a thermal bremsstrahlung plus emission line model to simulate charge exchange. The column density of absorbing HI used in the models was fixed to be $N_H = 10^{13}$ cm^{-2}, the column expected for the line of sight to the comet from Earth through interplanetary space. Although HI is an efficient absorber and scatterer of x-rays, at this low a column density the goodness of fit was insensitive to the value of N_H, except at energies below 250 eV, where the CXO effective area is rapidly decreasing and the fits are poor in any case.

Thermal bremsstrahlung and power law models do not fit the CXO spectrum (*31*). The best-fit bremsstrahlung model, with reduced $\chi\nu^2 \geq 12$, is illustrated in Web fig. 2A (*23*). A four-emission-line model, with variable line center energy, line width, and a small underlying Brem continuum (Web fig. 2B) produced a $\chi\nu^2$ of 1.08, with a strong emission feature near 0.56 keV and smaller features at 0.32, 0.40, and 0.67 keV. The energies of the four-line centers agree with those expected for line emission from hydrogen and helium-like oxygen and carbon ions, as produced after charge exchange from cometary neutrals to oxygen and carbon ions stripped of all or all but one electron (*32*). A similar model, but with the line width fixed to the reported instrument resolution (Web fig. 2C), produced the best $\chi\nu^2$ of 0.99 for 80

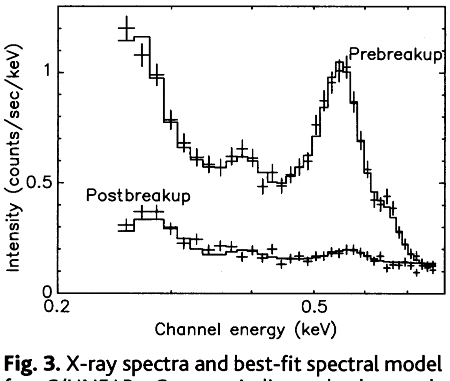

Fig. 3. X-ray spectra and best-fit spectral model for C/LINEAR. Crosses indicate background-corrected ACIS-S observations, both before (14 July 2000) and after (1 August 2000) breakup. Solid lines indicate best-fit six-line instrumental width + thermal bremsstrahlung emission model, convolved with the ACIS-S instrument response. The ACIS-S back-illuminated CCD has an intrinsic linewidth of 110 eV FWHM, yielding emission lines that are well modeled using 50 eV gaussian line profiles; features much narrower than this are not statistically significant.

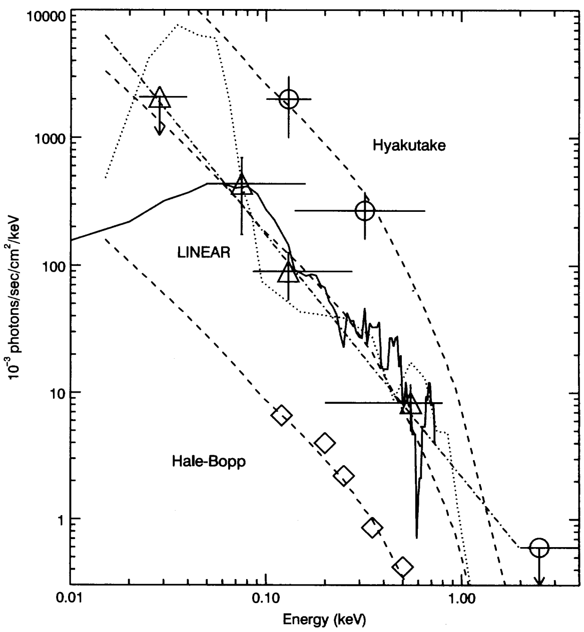

Fig. 4. Multiwavelength photometry of C/LINEAR (Δ) using the total CXO and EUVE count rates on 14 July 2000. The ROSAT/XTE results from C/Hyakutake on 26 to 28 March 1996 [circles (*1*)] and the BeppoSAX results from comet C/Hale-Bopp on 10 to 11 September 1996 [diamonds (*4*)] have been plotted for comparison. Dashed lines denote best-fit 0.30 keV thermal bremsstrahlung models; solid line denotes predicted C/LINEAR spectrum for the best-fit CXE model from Wegmann *et al.* (*9*); dash-dotted line denotes best-fit C/LINEAR power law model, $dN/dE \sim E^{-1.9}$; and dotted line denotes best-fit C/LINEAR Raymond-Smith solar abundance plasma model, with kT = 0.22 keV.

degrees of freedom (dof), and required six lines with energies at 320, 400, 490, 560, 600, and 670 eV. The additional lines are most probably due to CXE emission from N^{+7}.

At SNR about four times lower than the 14 July results, the spectrum obtained on 1 August 2000 is more difficult to interpret (Fig. 3). Nevertheless, applying the best-fit prebreakup spectral models, we find a good fit using three lines at 330, 380, and 570 eV + a thermal continuum, demonstrating the constancy of the emission mechanism. The amplitude of the O^{+7} 570 eV line versus the continuum is reduced by a factor of 2.5 compared to the 14 July spectrum.

The CXO ACIS-S spectra show evidence of line emission at the appropriate energies for hydrogen-like and helium-like C, N, and O solar wind ions, and do not match the continua expected for power law or bremsstrahlung emission. Extending the spectrum to lower energies by addition of the EUVE photometric points yields a spectrum rising toward a maximum flux density at ~0.10 keV, in agreement with the CXE model prediction for comet 2P/Encke 1997 (*2*) (Fig. 4). The discrete multiline + Brem model is the best fit to the entire spectral dataset, before and after breakup. Some continuum is required to reproduce the observed spectrum, though; we suspect that we have detected the maximum number of lines statistically possible in our 200 to 800 eV moderate resolution spectrum, given the ACIS instrument linewidth of ~ 0.1 keV, and the continuum is simply the blending of many weaker lines—in the same fashion that the first low-spectral resolution measurements of cometary x-ray emission produced pure continuum models (Fig. 4). The strong O^{+7} line found at 560 eV may have been detected at the 2σ level in the ROSAT PSPC spectrum of C/Levy 1990XX (*3*) and the BeppoSAX spectrum of C/Hale-Bopp 1995 O1 (*4*).

Assuming the CXE model of Cravens (*9*), we have $L_x \sim 4.0 \times 10^{-21} * N_{neutral} * N_{SW} * V$ erg s^{-1}. Using a spherical volume V of radius 100,000 km, spherical gas outflow at $v_{gas} = 0.8$ km s^{-1} and $Q_{gas} = 3 \times 10^{28}$ s^{-1} (Table 1) and a SOHO solar wind density outside the bowshock of ~ 30 cm^{-3}, we find a total x-ray luminosity for the comet of ~2×10^{15} erg s^{-1}, consistent with the observed CXO and EUVE luminosities. The bulk of the luminosity is emitted in the 0.02- to 0.70-keV energy range (Fig. 4). Using a charge exchange cross section of 3×10^{-15} cm^2 (*9*) and assuming spherical outflow for C/LINEAR with gas production rate ~ 3×10^{28} mol s^{-1} (*19, 20*), we find $\tau_{CXE} \sim 1$ for charge exchange at 300 km from the nucleus, whereas the minimum CXO resolution element has width ~10″ or 4000 km. Thus, the observed emission from the comet was optically thin to charge exchange except in the central PSF containing the nucleus; this region accounted for less than 0.1% of the total observed emission from the comet.

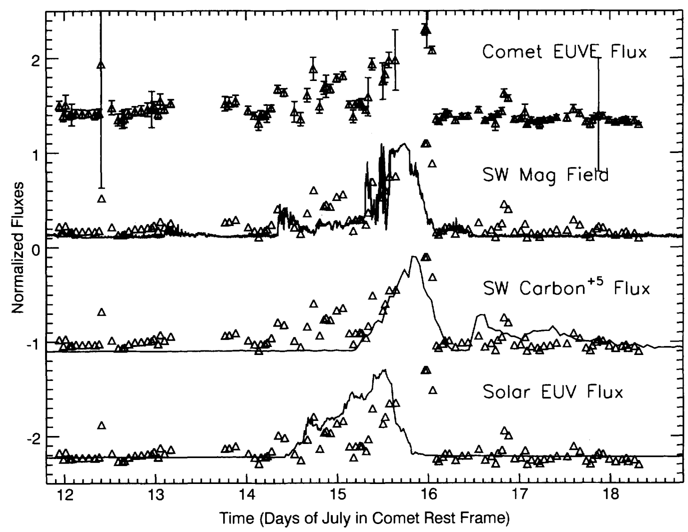

Fig. 5. EUVE scanner telescope 0.09- to 0.25-keV (Lexan B) light curve for C/LINEAR (Δ), taken contemporaneously with the CXO observations. All error bars are $\pm 1\sigma$. Also plotted are the WIND total magnetic field B_{total}, the ACE ULEIS solar wind $C^{+5} > 1$ MeV/nucleon flux, and the SOHO solar EUV flux. The sharp upturn in the solar wind flux and magnetic field starting on 14 July 2000 is due to an extremely strong solar flare. The C^{+5} flux measured at Earth has been shifted by +0.7 days, the delay expected due to Carrington rotation. The magnetic field measurements have been shifted by −0.3 days; this delay is appropriate for an impulsive event broadcast from the solar surface that is not tied to the solar rotation, propagating at >900 km/s. The solar EUV flux has <8 min delay between the comet and Earth.

Table 2. Predicted and observed light curve phase shifts using the simple latitude independent model. The estimated time shifts assume solar wind velocity as measured near-Earth. Positive time shifts imply that the solar wind impulse happens at Earth first, comet next. Negative time shifts imply the solar wind boundary hits comet first, Earth next.

Comet	Time of impulse (00:00H UT)	Δt_{long} (days)	Δt_{radial} (days)	Δt_{total} (days)	$\Delta t_{observed}$ (days)
Hyakutake	27 Mar 1996	−0.23	+0.032	−0.20	+0.24
Hale-Bopp	11 Sep 1996	−4.60	+5.9	+1.30	+1.4
Encke	7 Jul 1997	−0.26	+0.093	−0.17	−0.1
TT	29 Jan 1998	−2.31	+0.37	−1.94	−2.5
LINEAR S4	15 Jul 2000	+1.2	−0.30 to −0.50	+0.9 to +0.7	−0.25

However, a survey of published CXE spectral line shape predictions does not agree with the 14 July 2000 spectrum; the three line ratios of 2.3:4.5:1 for the 400-, 560-, and 670-eV lines are not as predicted by Häberli *et al.* (*10*), Wegmann *et al.* (*11*), or Kharchenko and Dalgarno (*12*). All of these models use simplifying assumptions concerning the behavior of the captured electron in order to make the emission calculation tractable, or assume nominal solar wind composition. Recent laboratory work (*32, 33*) has shown that the observed low-energy line ratios depend strongly on the solar wind and coma gas densities and interaction energies: different angular momentum states than nominal are populated in the excited capturing ion at high solar wind velocities, and in the collision-dominated regimes present in high-activity comets near the nucleus. The possible correlation of a radially propagating solar wind magnetic field with the x-ray light curve suggests that the hybrid plasma-wave emission mechanism of Bingham *et al.* (*13, 14*) may best describe the phenomenon. On the other hand, the change in the O^{+7} CXE line strength from 14 July to 1 August suggests that the solar wind composition may have varied substantially from solar abundances during the 14 and 15 July flare.

The EUVE 0.09- to 0.28-keV (Lexan B) lightcurve for the comet from 11 July 2000 to 18 July 2000, corrected for variable Earth-comet distance, shows two features (Fig. 5): a gently declining baseline of ~0.10 counts per second (cps) from 11 to 18 July, trending with the decreasing gas production rates (*19, 20*), and a large impulse, ramping up over 1 day (14 and 15 July 2000) to a value of 0.80 cps, and then ending in a rapid decay ($\tau \sim 1$ hour). A lightcurve for the CXO observations, created by binning the 4 hours of 200- to 800-eV 14 July observations in a 100,000-km radius aperture into 20 discrete intervals, shows a generally increasing trend throughout, from 0.8 to 1.5 cps, in good agreement with the EUVE lightcurve trend for the same time period.

On 26 to 28 July 2000, in between our first and last CXO observations, C/LINEAR disintegrated into a multitude of fragments (*34, 35*), with a concomitant drop in gas and dust production. Our second CXO spectrum taken 1 August 2000 (Fig. 3) shows a large drop in x-ray emission rate, by a factor of about 4, but still a clear detection above background of the 560-eV line. Unfortunately the gas and dust production rates decreased by about the same amount, a factor of 8, from the production rates measured early in July 2000 (*36*), making it difficult to easily separate their effects on the x-ray emission. Assuming an effect from Q_{gas} alone, we have $L_x \sim Q_{gas}^{0.67}$.

A large solar flare was detected at Earth on 14 and 15 July 2000. The time delay observed between the flare arriving at Earth (as measured by the near-Earth ACE, SOHO, and WIND spacecraft) and the observed x-ray outbursts at the comet can be predicted by assuming a latitude independent solar wind flow, a quadrupole solar magnetic field, and propagation of the sector boundaries radially at the speed of the solar wind, and axially with period 1/2 * solar rotation period of 28 days

$$\Delta t_{total} = \Delta t_{CR} + \Delta t_r = \frac{(longitude_{comet} - longitude_{Earth})}{14.7 \text{ deg/day}} + \frac{(r_{comet} - r_{Earth})}{400\ km/\text{sec} \cdot 86400 \text{ sec}/day}$$

C/LINEAR does not fit this model, however, using the SOHO solar wind proton fluxes, as for previous comets (Table 2) (*1, 2*). The time delay expected for the Carrington rotation model (Fig. 5) does predict a large outburst from the proton flux and magnetic field on 14 and 15 July 2000, but also predicts an equally large outburst earlier on 14 July and another on 16 July that were only weakly detected.

Unlike our previous observations of comets (*1, 2, 5*), the solar wind proton flux and solar wind magnetic field demonstrated different trends during our observations, allowing us to determine the importance of the flux and magnetic field separately. We can rule out any solar x-ray scattering mechanism, because the large increase in solar flux seen on 14 and 15 July is not coincident with the comet's emission. The best fit to the x-ray lightcurves using our SOHO and WIND measurements is the solar wind magnetic field with a radial delay only (Fig. 5), predicting the large 14 and 15 July event and a small early 14 July event, but not a small event in mid–16 July. One explanation for this result is that the flare consisted of a brief, impulsive event in the solar atmosphere emitted into a large solid angle, and not tied to the solar rotation.

On the other hand, as for previous comets, it is hard to understand the role of the solar wind magnetic field in the emission, because extensive x-ray emission is found outside the bowshock, with no discontinuity marking the magnetic field enhancement inside the shock. We have also found the same spectral signature in and out of the flare, arguing that the emission mechanism should be the same for all comets at all times, including normal sector boundary crossings. Because there is the signature of CXE created line emission in our data, and the simplest CXE models depend on the solar wind minor ion flux and the comet neutral gas flux alone, an alternative explanation is that the solar wind proton flux is not a good measure of the solar wind minor ion flux in the flare experienced by C/LINEAR. Examination of the ACE ULEIS ultrasoft ion spectroscopy data for H, He^4, C, O, Ne, Fe, taken at L1, seemed to bear this out: the solar wind fluxes for H and the heavier ions at low energy are identical, whereas the highest energy minor ion fluxes, >1 MeV/nucleon, have a pronounced peak on 14 and 15 July 2000 not found in the proton curves. The peak at higher energies is especially pronounced for He and Fe; the relative height of the peak may explain the unusual ratio of C:N:O lines found in our spectra. Shifting the measured C^{+5} flux for the expected Carrington rotation delay produces agreement with the observed EUVE count rates (Fig. 5). If true, why the proton-minor ion correlation breaks down for a flare versus a sector boundary crossing is not clear, and is most probably due to the detailed physics involved with solar flare generation. In either case, the usefulness of cometary x-ray emission for understanding the solar wind environment in all parts of the solar system is evident (*37*).

References and Notes

1. C. M. Lisse *et al.*, *Science* **274**, 205 (1996).
2. C. M. Lisse *et al.*, *Icarus* **141**, 316 (1999).
3. K. Dennerl *et al.*, *Science* **277**, 1625 (1997).
4. A. Owens *et al.*, *Astrophys J.* **493**, 47 (1998).
5. C. M. Lisse *et al.*, *Earth Moon Planets* **77**, 283 (1999).
6. V. A. Krasnopolsky *et al.*, *Science* **277**, 1488 (1997).
7. M. J. Mumma, V. A. Krasnopolsky, M. J. Abott, *Astrophys. J.* **49**, L125 (1998).
8. V. A. Krasnopolsky, M. J. Mumma, *Astrophys. J.* **549**, 629 (2001).
9. T. E. Cravens, *Geophys. Res. Lett.* **24**, 105 (1997).
10. R. M. Häberli *et al.*, *Science* **276**, 939 (1997).
11. R. Wegmann *et al.*, *Planet. Space Sci.* **46**, 603 (1998).
12. V. Kharchenko, A. Dalgarno, *J. Geophys. Res.* **105**, 18351 (2000).
13. R. Bingham *et al.*, *Science* **275**, 49 (1997).
14. R. Bingham *et al.*, *Astrophys. J. Suppl. Ser.* **127**, 233 (2000).
15. T. G. Northrop *et al.*, *Icarus* **127**, 246 (1997).
16. T. G. Northrop, *Icarus* **128**, 480 (1997).
17. M. Uchida *et al.*, *Astrophys. J.* **498**, 863 (1998).
18. C. M. Lisse *et al.*, in preparation.
19. T. L. Farnham *et al.*, *Science* **292**, 1348 (2001).
20. D. Bockelée-Morvan *et al.*, *Science* **292**, 1339 (2001).
21. CXO observations of comet C/LINEAR were obtained using the ACIS-S CCD spectral array, which combines the ability to image x-rays with platescale of 0.5″/pixel and to produce moderate resolution spectra [$\Delta E \sim 110$ eV full-width at half maximum (FWHM), $\Delta E_{gaussian} = 49$ eV] from 0.25 to 0.8 keV. The observations consist of a list of time-tagged detections of individual photon pulse heights and spatial locations. CXO was able to follow the comet's nonsidereal motion using multiple pointings, and the target was centered in the back-illuminated CCD chip S3, the most optimal for x-ray spectroscopy. Using a preliminary version of the "sso_freeze" algorithm, part of the Chandra Interactive Analysis of Observations (CIAO) software, we constructed a comet image remapped into a coordinate system moving with the comet (*38*). To create light curves, a circular source aperture of 3.7′ radius was chosen in CIAO, and several background apertures were extracted >4′ away from the comet's diffuse emission and toward the outer edge of the chip (*39*). Spectra were extracted in an identical fashion, and the effect of energy-dependent instrument sensitivity was removed using the effective areas given in the CXO on-orbit measured instrument response matrices. Upon examination of the extracted spectra, only photons of energy 200 to 800 eV were found to be statistically significant against the sky and instrumental backgrounds. Comparison of the EUVE 0.09- to 0.25-keV images and CXO images demonstrated that the comet overfilled the entire S3 field-of-view, and all absolute CXO count rates have been corrected for vignetting using aperture photometry curves from the two cameras.
22. H. Mikunz, personal communication.
23. Supplementary material is available at www.sciencemag.org/cgi/content/full/292/5520/1343/DC1
24. The EUVE measurements were taken using the three "scanner" co-aligned telescopes. Each of these is mounted perpendicular to the EUVE spin axis, and supports broadband [Lexan/Boron ("Lexan B") at 0.09 to 0.28 keV (44 to 140 Å), Al/Ti/C ("Al/Ti/C") at 0.05 to 0.16 keV (77 to 250 Å), and the Ti/Sb/Ti/Al ("Dagwood") at 0.02 to 0.04 keV (310 to 620 Å)] filter observations of astrophysical targets using a microchannel plate detector. SOHO measurements of the solar wind proton flux, solar soft x-ray flux, and solar wind magnetic field were obtained using the CELIAS instrument, with data obtained from www.usc.edu/dept/space_science/semdata97.htm. ACE ULEIS ultrasoft ion spectroscopy data for H, He^4, C, O, Ne, and Fe were found at http://sd-www.jhuapl.edu/ACE/ULEIS/spec_gadget.html. Our observations of C/LINEAR using the EUVE scanners and of the solar-terrestrial environment using the SOHO, WIND, and ACE spacecraft were performed in the same manner as used to observe comets Encke (*2*) and Hale-Bopp (*6*).
25. The bowshock is the region of the coma where the fluid solar wind, impinging on the much thicker cometary coma ionosphere, picks up enough coma mass ("mass loading") to abruptly slow down in a gentle shock while increasing markedly in density and magnetic field strength. The contact surface is the location in the coma inside of which ionic species and interplanetary magnetic field lines are excluded. The existence of both of these predicted regions in the cometary coma was verified during the in situ flybys of comet 1P/Halley 1986 by the Giotto and Vega spacecraft. For a good review of the flybys, see H. Reme *et al.* [*Astron. Astrophys.* **187**, 33 (1987)].
26. K. R. Flammer, in *Comets in the Post-Halley Era*, IAU Colloqium 121, Bamberg, Germany, 24 to 28 April 1989, R. L. Newburn, M. Neugebauer, J. Rahe, Eds. (Kluwer Academic, Dordecht, Netherlands, 1991), p. 1125.
27. M. Neugebauer *et al.*, *Astron. Astrophys.* **187**, 21 (1987).
28. M. Neugebauer *et al.*, *J. Geophys. Res.* **103**, 14587 (1998).
29. T. Mukai *et al.*, *Astron. Astrophys.* **187**, 129 (1987).
30. The location of the shock near the edges of the wings is typically, at most, a factor of 2 farther from the nucleus than at the subsolar point.
31. See Web table 1 (*23*).
32. The predicted energies for emission by an electron captured onto hydrogenic and heliogenic species was first published by R. L. Kelly [*J. Phys. Chem. Ref. Data* *16* (suppl. 1), 1371 (1987)]. The O^{+7} and O^{+8} lines have recently been confirmed in the laboratory, at the interaction energies present in the solar wind-comet system, by J. Greenwood *et al.* [*Astrophys. J.* **533**, L175 (2000)].
33. P. Beiersdorfer *et al.*, *Astrophys. J.* **549**, L147 (2001).
34. M. Kidger, *IAU Circular* **7467** (2000).
35. H. A. Weaver *et al.*, *Science* **292**, 1329 (2001).

36. D. G. Scheliecher, C. Eberhardy, *IAU Circular* **7455** (2000); personal communication (2001).
37. Although it is based on the overly simplified Wegmann model (*11*), a good discussion of how to interpret the x-ray spectra for variable solar wind flux and composition is given by N. A. Schwadron and T. E. Cravens [*Astrophys. J.* **544**, 558 (2000)].
38. We have used the cometary ephemerides (DE-405, mid-June 2000, epoch = 4 August 2000) of D. K. Yeomans *et al.* found at http://ssd.jpl.nasa.gov/horizons.html to target the comet and to remap our observations into a comet-centered reference frame. The estimated pointing uncertainties for the CXO and EUVE spacecraft are 1″ and 10″, respectively. The estimated ephemeris uncertainties for C/LINEAR are large, due to the large nongravitational (i.e., jet) forces created during the comet's prolonged breakup in July 2000, on the order of 10″ or so, and along with the 1′ HEW of the EUVE scanner telescopes, dominate the EUVE positional uncertainties of our observations. For the CXO observations, the limited number of detected photons (~13,000) restricted the effective detector resolution, due to statistical counting uncertainties, to pixels of 10″ extent.
39. E. Feigelson *et al.*, *Bull. Am. Astron. Soc.* **32**, 27.02 (2000), http://www.aas.org/publications/baas/v32n3/head2001/173.htm
40. The SOHO and WIND data were graciously provided by R. Lepping of NASA/Goddard Spaceflight Center and H. Ogawa of University of Southern California. The ACE data were provided courtesy of S. Nyland of Johns Hopkins University. We are grateful for the cometary ephemeredes of D. K. Yeomans *et al.*, found at the Jet Propulsion Laboratory Horizons website used to reduce our data. The optical images and photometry of C/LINEAR on 14 July 2000 was provided by H. Mikuz of the Crni Vrh Observatory, Slovenia. We thank the Chandra X-ray Center, especially R. Hain for reconstructing the comet images, and B. Stroozas and the EUVE Science Operations team for working with us to schedule the moving target observations. C.M.L. was supported in part by NASA Planetary Astronomy Program Grant No. NAGW188 and by observing grants NAG5-6141 and NAG5-6155. K.D. gratefully acknowledges support from the German Bundesministerium für Bildung, Wissenschaft, Forschung und Technologie (BMBF/DARA) and the Max-Planck-Gesellschaft. S.J.W. was supported by NASA contract NAS8-39073.

26 December 2000; accepted 24 April 2001

Imaging and Photometry of Comet C/1999 S4 (LINEAR) Before Perihelion and After Breakup

Tony L. Farnham,[1*] David G. Schleicher,[2] Laura M. Woodney,[2] Peter V. Birch,[3] Clara A. Eberhardy,[4] Lorenza Levy[5]

We analyzed photometric measurements and images of comet C/LINEAR before perihelion and after its breakup. Results from our photometry data include a lower limit of 0.44 kilometer for the radius of the nucleus before breakup, and a determination that it was depleted in carbon-chain molecules relative to most other comets. Our imaging and modeling results, which include a constraint on the rotational state of the nucleus, indicate that the disintegration likely started on 18 or 19 July 2000. The total mass detectable in the dust tail after the breakup was 3 × 10⁸ kilograms, comparable to one of the fragments in the Hubble Space Telescope images; we therefore infer that most of the comet's original mass is hidden in remnants between 1 millimeter and 50 meters in diameter.

Comet C/1999 S4 (LINEAR) passed its closest point to Earth, 0.364 AU, on 23 July 2000, 3 days before it reached perihelion. Coincidentally, the comet completely disintegrated within a few days of its closest approach to Earth. The timing of this event was ideal because astronomers taking advantage of the favorable geometric conditions to observe C/LINEAR were able to obtain measurements of the spontaneous disintegration of its nucleus. These measurements, combined with observations before and after the disruption, constitute a unique data set that can be used to investigate the structure and composition of the comet's nucleus as well as the processes contributing to the breakup. We observed C/LINEAR for 14 nights with narrowband photometry and obtained charge-coupled device (CCD) images on 36 nights.

Our photometric observations began on 5 December 1999, when the comet was 3.57 AU from the Sun, and concluded on 1 August 2000, about 1 week after the comet's disintegration (Table 1). Data were obtained using a photoelectric photometer equipped with pulse-counting electronics with the 72-inch (1.8-m) Perkins and 42-inch (1.1-m) Hall telescopes at Lowell Observatory. Emission bands of OH, NH, CN, C_2, and C_3 were isolated with narrowband filters, and the reflected continuum was evaluated by measurements of dust grains at wavelengths of 345, 445, and 526 nm (*1*). Standard procedures were followed in data acquisition, reduction, and computation of gas (Q) and dust-equivalent [$A(\theta)f\rho$] production rates (*2, 3*).

The heliocentric distance (r_H) dependences of the derived production rates for the individual observations are given in Fig. 1; mean production rates for each night are shown in Table 1. CN, the best-measured gas species, exhibited the expected increase in Q as r_H decreased from 3.56 to 2.18 AU, before leveling or slightly dropping between 1.15 and 0.80 AU. As originally reported (*4*), the three consecutive nights in June show considerable variability, with all gas species peaking on 11 June with values more than 40% greater than on the surrounding nights. This minor outburst, confirmed by monitoring data from the Solar Wind Anisotropies (SWAN) instrument onboard the Solar and Heliospheric Observatory (SOHO) (*5, 6*), was one of a series of sporadic outbursts or partial fragmentations that preceded the disintegration of the comet. The SOHO record also indicates that our 13 July measurements were obtained shortly after a minor outburst, so they should be near the baseline level of comet activity. Therefore, we fit a quadratic function to the CN data (Fig. 1), excluding the 11 June outburst and the late July data taken after the breakup of the nucleus. For comparison, we then transposed the CN production curve to the plots of the other species in Fig. 1 (*7*).

The transposed CN curves are consistent with the measured Q values of OH and C_2 at large r_H, with CN and C_2 increasing by a factor of ~18 between December 1999 and July 2000 while OH increased by a factor of 28. In contrast, the derived dust production increased by less than a factor of 3 during the apparition and was essentially constant as r_H decreased from 3.56 to 2.18 AU, an interval in which the gas production increased by a factor of 6. These characteristics of the dust imply that the measured values of $A(\theta)f\rho$ at $r_H > 2$ AU were not true measures of ongoing dust production, but rather were dominated by dust that was released before C/LINEAR's discovery and remained in the comet's coma as a result of the combination of low outflow velocity and small radiation pressure at large r_H. This scenario is consistent with that expected for a dynamically new comet (*8*), which typically exhibits excessive activity at $r_H > 5$ AU and then brightens more slowly as this activity declines (*9*). As a

[1]Department of Astronomy, University of Texas, Austin, TX 78712, USA. [2]Lowell Observatory, 1400 West Mars Hill Road, Flagstaff, AZ 86001, USA. [3]Perth Observatory, Walnut Road, Bickley 6076, Western Australia. [4]Department of Astronomy, University of Washington, Physics/Astronomy Building, Stevens Way, Box 351580, Seattle, WA 98195, USA. [5]Department of Physics and Astronomy, Northern Arizona University, Box 6010, Flagstaff, AZ 86011, USA.

*To whom correspondence should be addressed. E-mail: farnham@astro.as.utexas.edu